Experimental report

15/09/2018

Proposal: **7-04-156** **Council:** 4/2017

Title: Quantised translational states of atomic He confined inside a nearly spherical cage: the endofullerene He@C60

Research area: Physics

This proposal is a new proposal

Main proposer: **Anthony J. HORSEWILL**

Experimental team: George BACANU
Gabriela SITINOVA
Anthony J. HORSEWILL

Local contacts: Stephane ROLS

Samples: C60
3He@C60
4He@C60

Instrument	Requested days	Allocated days	From	To
IN4	6	6	28/05/2018	04/06/2018

Abstract:

Highly innovative 'molecular surgery' techniques have been developed in recent years to synthesise small molecule endofullerenes in which the molecular cage of C60 completely encloses and entraps a quantum rotor such as H2, H2O or HF. The physical entrapment provides a nanolaboratory environment in which to study the isolated molecule and to exploit its physical properties. In this new proposal we are shifting emphasis to the study of entrapped atomic species. In particular 3He is highly receptive to NMR with the capacity to be prepared in a hyperpolarised nuclear spin state. Yet to develop laser-pumping hyperpolarisation protocols and exploit the possibilities that such a spin system far from equilibrium would provide, a detailed characterisation of the translational energy levels of the He atom inside its cage is required. This is uniquely available using neutron scattering.

Introduction :

Endofullerenes are composed of supramolecular complexes, each of which consists of a small (endohedral) atom/molecule enclosed by a fullerene (C_{60}) cage. Endofullerenes offer an ideal particle in a box system to directly observe translational (atomic) quantization, which leads to energy levels sensitive to the intermolecular interaction potential.

The aim of this study was firstly to observe transitions arising purely from atomic translational quantization due to confinement of a helium atom inside an almost spherical cage. And secondly to obtain a detailed characterisation of the translational energy levels, to be used for further NMR applications of hyperpolarised helium in $^3He@C_{60}$. From the energy level structure a derivation of the confining potential for the $He@C_{60}$ complex should be feasible.

Experimental :

224 mg of $^3He@C_{60}$ (4.4% filling factor) was transferred to a thin rectangular (∼ 1cm x 1cm) aluminium foil cell and then put in the orange cryostat for measuring.

175 mg of $^4He@C_{60}$ (26.1% ff.) was transferred to a thin rectangular (∼ 1cm x 1cm) aluminium foil cell and then put in the orange cryostat for measuring. The same procedure was done for 739 mg of empty C_{60}.

He@C$_{60}$ NMR Results:

From ^{13}C NMR measurements using the C_{60} cage carbons the ratios of $He@C_{60}$, C_{60} and $H_2O@C_{60}$ were obtained:

For $^3He@C_{60}$ sample the ratios are $^3He@C_{60}$: $H_2O@C_{60}$: C_{60} = 0.2 : 4.4 : 95.4.

For $^4He@C_{60}$ sample the ratios are $^4He@C_{60}$: $H_2O@C_{60}$: C_{60} = 0.1 : 26.1 : 73.8.

INS Results :

From ref.[1] the total scattering cross sections for "thermal" neutrons (10-100 meV) are: $\sigma_{^1H} = 81.7$ barn, $\sigma_{^3He} = 5.6$ barn, $\sigma_{^4He} = 1.2$ barn and $\sigma_{^{16}O} = 4.2$ barn. With those values the total scattering cross section for H_2O would be $\sigma_{H_2O} = 167.6$ barn. With these values in mind and the relative ratios of $^3He@C_{60}$:$H_2O@C_{60}$ and $^4He@C_{60}$:$H_2O@C_{60}$, the following ratios of scattering power were obtained:

$\frac{\sigma_{^3He} \cdot \text{ratio}_{^3He}}{\sigma_{H_2O} \cdot \text{ratio}_{H_2O}} = \frac{5.6 \cdot 4.4\%}{167.6 \cdot 0.2\%} = \frac{24.64}{33.52} = \frac{1}{1.36}$ and $\frac{\sigma_{^4He} \cdot \text{ratio}_{^3He}}{\sigma_{H_2O} \cdot \text{ratio}_{H_2O}} = \frac{1.2 \cdot 26.1\%}{167.6 \cdot 0.1\%} = \frac{31.32}{16.76} = \frac{1}{0.53}$

Thus $^3He@C_{60}$ should scatter almost as much as $H_2O@C_{60}$ whereas $^4He@C_{60}$ should scatter about twice as much as $H_2O@C_{60}$, and this is what is being observed in the INS spectra in the sections below.

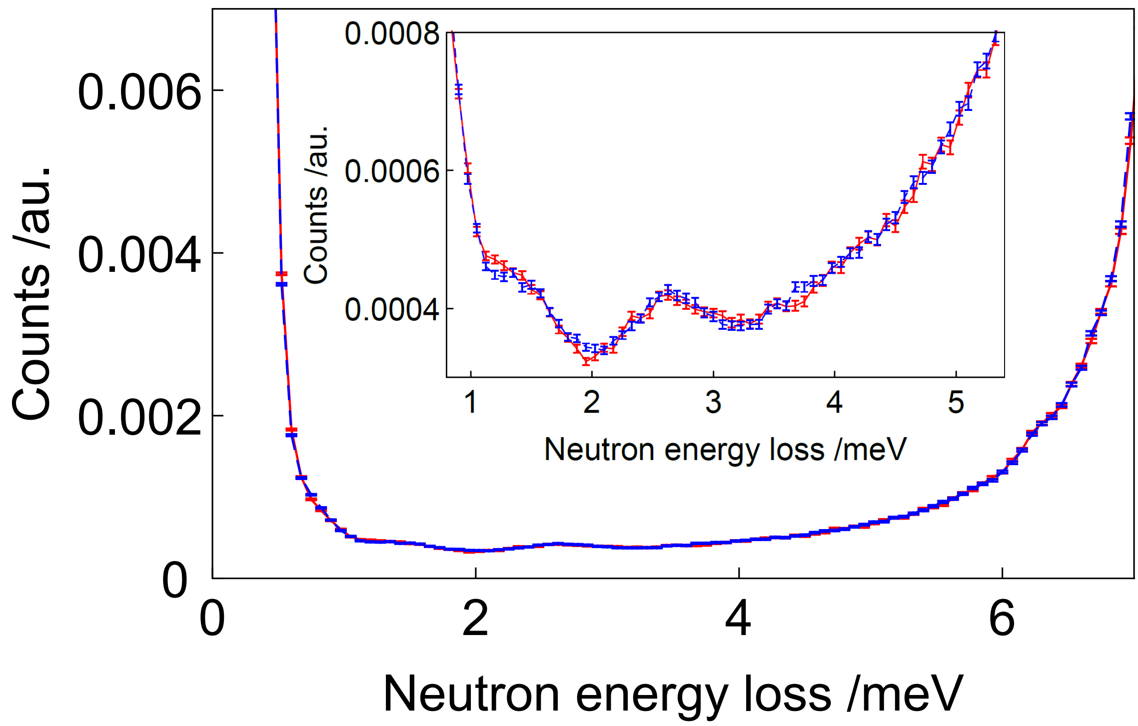

Figure 1: Relevant INS spectrum of $^3He@C_{60}$(red) and $^4He@C_{60}$(blue dashed) with no background subtraction, scattered intensity against neutron energy loss. Incident neutron wavelength 3.2 Å at 1.6 K acquiring for 16 h $^3He@C_{60}$ and 22 h $^4He@C_{60}$.

Unfortunately the ball bearings of the background choppers on IN4c crashed when we were acquiring the empty cell background for 1.6 Å and 3.2 Å so the background subtraction for these wavelengths was faulty. 3.2 Å empty cell measurement was completely unusable but 1.6 Å was acceptable in the lower energy part of the spectrum but quite bad in the high energy transfer regime.

The 3.2 Å wavelength allows to see in the low energy part of the spectrum but because a good background subtraction was not possible, the pure ^{3}He@C$_{60}$ and ^{4}He@C$_{60}$ INS spectra are shown in fig. 1. It can be seen that there is no difference between the two spectra, concluding that there is no translational transition arising from either ^{3}He@C$_{60}$ or ^{4}He@C$_{60}$ in this energy regime.

^{3}He@C$_{60}$ INS Results :

Fig. 2 bottom contains the INS spectrum of ^{3}He@C$_{60}$(neutron wavelenght 2.2 Å). The spectrum was fitted with 5 Gaussian peaks, 4 of them come from H$_2$O@C$_{60}$ (green peaks marked with asterisk)[2] and one comes from the ^{3}He@C$_{60}$ at 11.77 ± 0.02 meV (red peak).

The same experiment was repeated using a neutron wavelength of 1.6 Å, see fig. 2 top. On the figure there is another very broad feature centred around 20 meV but no obvious structure can be seen here and a fit with gaussian peaks was unsuccessful, we expect this feature to arise from a combination of H$_2$O@C$_{60}$ and ^{3}He@C$_{60}$ peaks. The broadness comes from overlap with other H$_2$O@C$_{60}$ peaks in this region and the very small ratio of it in the sample buries the peaks under the noise.

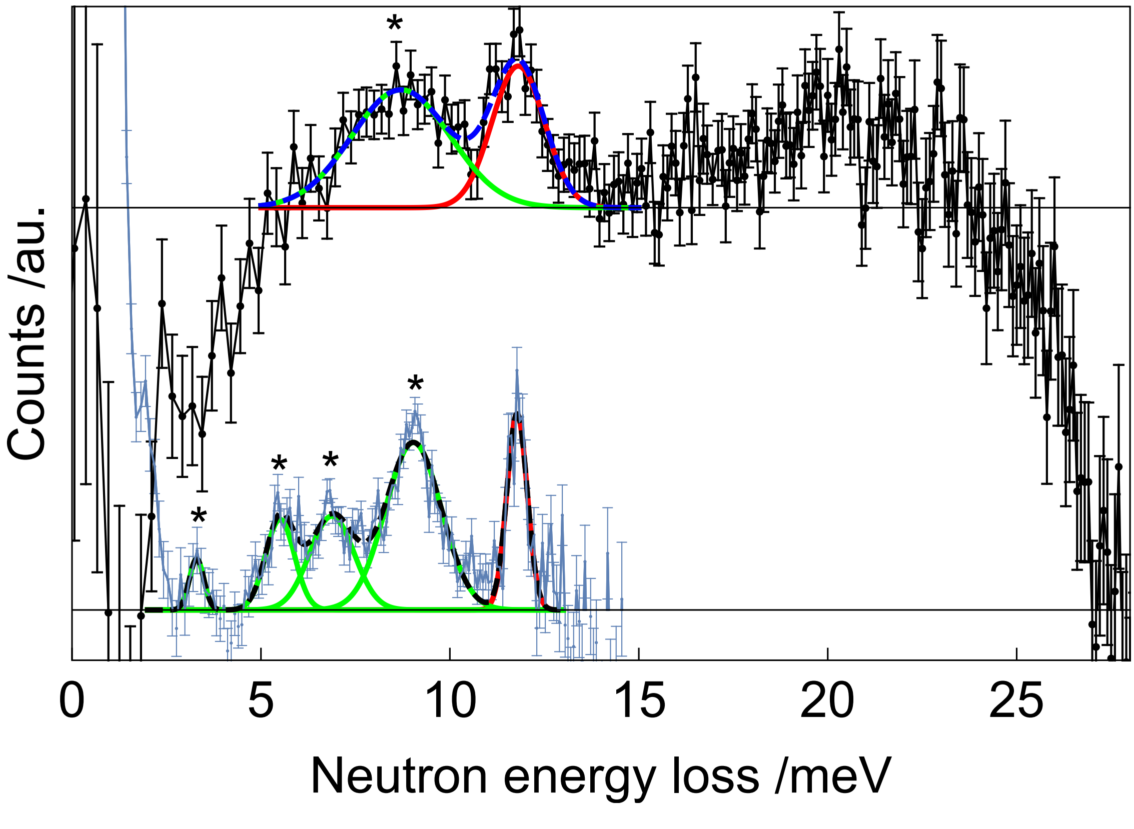

Figure 2: Relevant INS spectrum of ^{3}He@C$_{60}$, scattered intensity against neutron energy loss. Black (top) spectrum: Incident neutron wavelength 1.6 Å at 1.6 K acquiring for 8 h, Blue (bottom) spectrum: Incident neutron wavelength 2.2 Å at 1.6 K acquiring for 41 h. Straight horizontal lines represents the zero line for the respective spectrum. H$_2$O@C$_{60}$ peaks are marked with an asterisk.[2] ^{3}He@C$_{60}$ peak is at 11.77 ± 0.02 meV.

^{4}He@C$_{60}$ INS Results :

The scattering power argument above implies the peak intensities for H$_2$O@C$_{60}$ in the ^{4}He@C$_{60}$ sample are twice as weak than for ^{3}He@C$_{60}$ and a fit for all the H$_2$O@C$_{60}$ peaks was not possible. Only the region with the most intense peaks was fitted with 2 gaussian peaks, one for H$_2$O@C$_{60}$ (green marked with asterisk) and one for ^{3}He@C$_{60}$ (red) at 9.85 ± 0.02 meV, see fig. 3 bottom. A straight line was fitted for the region around the peaks to account for the raised and tilted baseline with a line equation of : $0.00003036 - 1.816 * 10^{-6}x$. The same experiment was repeated using a neutron wavelength of 1.6 Å to explore the higher energy regions of the spectrum, see fig. 3 top. Same argument as for ^{3}He@C$_{60}$ above for the broad peak centred around 20 meV.

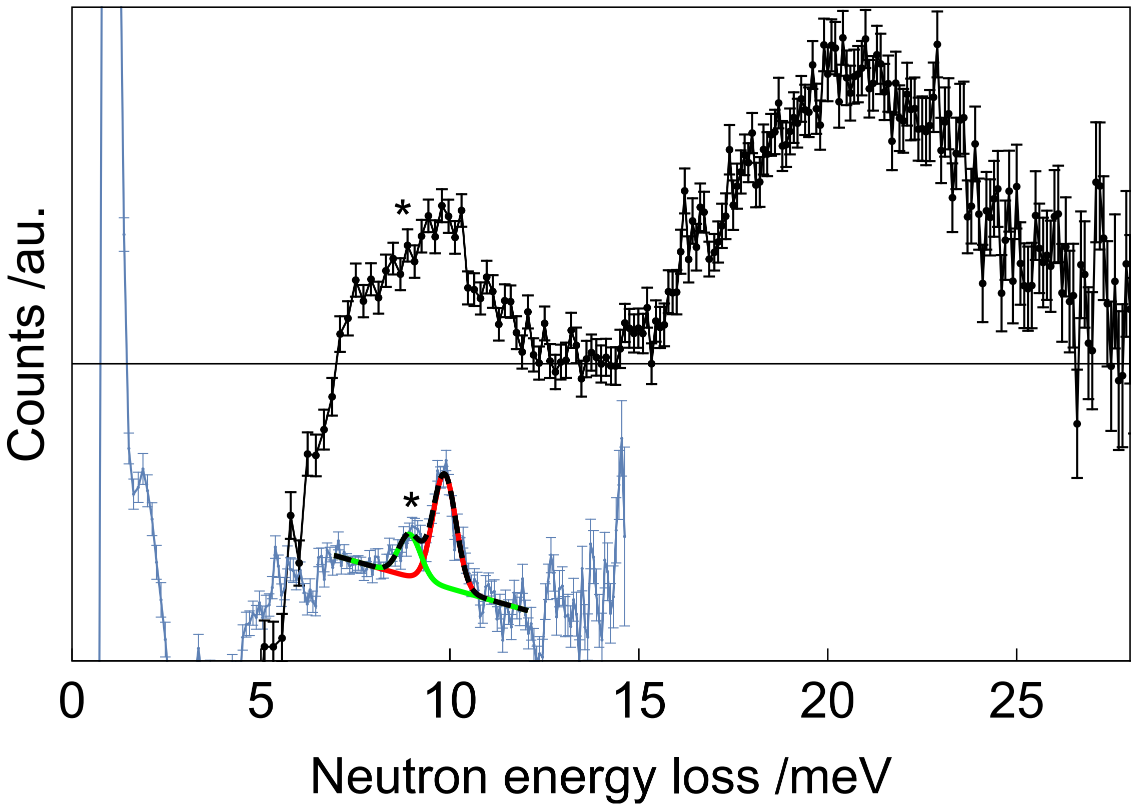

Figure 3: Relevant INS spectrum of $^4He@C_{60}$, scattered intensity against neutron energy loss. Black (top) spectrum: Incident neutron wavelength 1.6 Å at 1.6 K acquiring for 8 h, Blue (bottom) spectrum: Incident neutron wavelength 2.2 Å at 1.6 K acquiring for 40 h. Straight horizontal lines represents the zero line for the respective spectrum. $H_2O@C_{60}$ peaks are marked with an asterisk.[2] $^4He@C_{60}$ peak is at 9.85 ± 0.02 meV.

He@C$_{60}$ confining potential :

Using the observed transitions and a perturbed harmonic oscillator model to get the quantised translational energy levels of He@C$_{60}$ the following confining potential was obtained:

$V^{C_{60}-He} = (0.4241\,J\,m^{-2}) \cdot r^2 + (0.3922 \cdot 10^{20}\,J\,m^{-4}) \cdot r^4$

From infra red data on $H_2@C_{60}$ a potential for the C$_{60}$−H interaction was obtained using a Lennard-Jones potential for the C−H interaction and summing over all 60 carbon atoms.[3] A polynomial approximation (up to 6th order) of the C$_{60}$−H interaction potential was made and is given below:[4]

$V^{C_{60}-H} = (0.12\,J\,m^{-2}) \cdot r^2 + (0.2 \cdot 10^{20}\,J\,m^{-4}) \cdot r^4 + (0.1 \cdot 10^{40}\,J\,m^{-6}) \cdot r^6$

Conclusion :

Inelastic neutrons scattering measurements on He@C$_{60}$ have made possible the assignment of pure translational transitions arising from the confinement of helium inside the C$_{60}$ cage. Even if the experimental spectra were not ideal, a perturbation applied to the 3D isotropic harmonic oscillator has given an initial approximation to the confining potential for helium inside the C$_{60}$ cage. This potential is comparable to the one obtained for a hydrogen atom inside C$_{60}$ for the $H_2@C_{60}$ system. However, the comparison between the two potentials is rather unexpected because helium inside C$_{60}$ should have a flatter potential, due to its inertness as a noble gas there should be very little interaction with the inside of C$_{60}$. More measurements will be performed to get a detailed description of the energy levels in order to confirm this observation.

References:

[1] S. W. Lovesey, *Theory of Neutron Scattering from Condensed Matter. Volume I: Nuclear Scattering*, Oxford University Press, New York, 1984.

[2] K. S. K. Goh, M. Jimenez-Ruiz, M. R. Johnson, S. Rols, J. Ollivier, M. S. Denning, S. Mamone, M. H. Levitt, X. Lei, Y. Li, N. J. Turro, Y. Murata and A. J. Horsewill, *Phys. Chem. Chem. Phys.*, 2014, **16**, 21330-21339.

[3] M. Xu, F. Sebastianelli, B. R. Gibbons, Z. Bačić, R. Lawler and N. J. Turro, *The Journal of Chemical Physics*, 2009, **130**, 224306.

[4] S. Mamone, *Ph.D. thesis*, University of Southampton, School of Chemistry, 2011.